Molecular Plant Pathology

WILEY

Molecular Plant Pathology

ORIGINAL ARTICLE OPEN ACCESS

The *Valsa mali* Effector VmSR1 Accelerates the Degradation of Tudor-SN2 to Suppress RNA Silencing and Plant Immunity

Tao Jiang[1] | Chengli Wang[1] | Mian Zhang[1] | Yongli Qiao[2] | Zhensheng Kang[1] | Lili Huang[1]

[1]State Key Laboratory for Crop Stress Resistance and High-Efficiency Production, College of Plant Protection, Northwest A&F University, Yangling, Shaanxi, China | [2]Shanghai Key Laboratory of Plant Molecular Sciences, College of Life Sciences, Shanghai Normal University, Shanghai, China

Correspondence: Zhensheng Kang (kangzs@nwafu.edu.cn) | Lili Huang (huanglili@nwsuaf.edu.cn)

Received: 26 January 2025 | **Revised:** 20 April 2025 | **Accepted:** 6 May 2025

Funding: This work was supported by Shaanxi Provincial Government (F1020221012).

Keywords: apple | miRNA | RNA silencing suppressors | Tudor-SN | *Valsa mali*

ABSTRACT

The apple Valsa canker caused by *Valsa mali* is one of the most destructive trunk diseases in apple production and disease management. Understanding the interaction between the pathogen and host is a critical foundation for developing durable disease control technologies. In this study, we showed that VmSR1 from *V. mali* can suppress the plant immune response and promote pathogen infection. VmSR1 associates with the Tudor staphylococcal nuclease 2 (TSN2) proteins in *Malus domestica* (apple), *Arabidopsis thaliana* and *Nicotiana benthamiana*, promotes degradation of TSN2 proteins, and suppresses the abundance of multiple miRNAs an Silencing of *TSN2* significantly reduced the abundance of miRNAs and weakened the resistance of apple leaves to *V. mali* as well as *N. benthamiana* to *Sclerotinia sclerotiorum*. These findings expand the understanding of the function of effectors as RNA silencing suppressors during host–pathogen interactions and deepen the understanding of effectors regulating host immunity.

1 | Introduction

The pathogen *Valsa mali* infects apple branches and trunks, causing branch dieback, and apple trees die in severe cases, seriously hindering the development of the apple industry. Several effectors have been reported to function during *V. mali* infection of apple trees. VmSpm1 can impair jasmonic acid (JA) signal transduction in apples, thereby enhancing the pathogenicity of pathogens (Meng et al. 2024). VmPR1c reduces the immune response by promoting the degradation of MdVQ29 (Han et al. 2024). Vm_04797 and Vm1G-1794 weaken plant disease resistance by interfering with autophagy in apple trees (Che et al. 2023; Sun et al. 2024). In addition, cell wall-degrading enzymes, toxins and sRNAs also play crucial roles in the pathogenesis of *V. mali* (Feng et al. 2023). For example, the VmR2-siR1 produced by *V. mali* is secreted into apple cells, where it suppresses the mRNA levels of *MdLRP14*, ultimately leading to enhanced plant susceptibility (Liang et al. 2024).

RNA silencing is a specific and efficient mechanism for mRNA degradation and protein translation regulation (McManus and Sharp 2002; Mao et al. 2007; Melnyk et al. 2011; Elbashir et al. 2001). The core participants in RNA silencing are small RNAs (sRNAs) with a length of 20–30 nucleotides, which bind to the Argonaute (AGO) protein to form an RNA-induced silencing complex (RISC) (Zhao and Guo 2022). *Arabidopsis* miR393 is induced by flg22, inhibits the expression of the target gene F-box family auxin receptor, activating the pathogen-associated molecular pattern (PAMP)-triggered immunity (PTI) response (Navarro et al. 2006). sRNAs can not only finely regulate the expression of the plant immunity-related genes in plants, but also directly act as disease resistance factors to induce gene

silencing of pathogens (Cai et al. 2018; He et al. 2021). Cotton can deliver its own miR159 and miR166 into the pathogenic fungus *Verticillium dahliae*, targeting HiC-15 and Clp-1, respectively, to inhibit pathogenicity (Zhang et al. 2016).

Conversely, pathogens counteract the plant RNA silencing by encoding effectors that interfere with the host RNA silencing pathway. The first RNA silencing suppressor protein, HC-Pro, was identified in poty viruses (Anandalakshmi et al. 1998). Since then, numerous viral suppressors such as CMV 2b, P19 and NS3 have been discovered (Brigneti et al. 1998; Qu and Morris 2002; Schnettler et al. 2008). Fungal RNA silencing inhibitors were first reported in the oomycete *Phytophthora sojae*, where two proteins, PSR1 and PSR2, exhibit RNAi inhibitory activity (Qiao et al. 2013). PSR1 interacts with the nuclear protein PINP1 to affect sRNA processing, whereas PSR2 interacts with the plant protein DRB4 to inhibit secondary siRNA synthesis (Zhang et al. 2019; Hou et al. 2019). *Puccinia graminis* f. sp. *tritici* protein PgtSR1 also affects host resistance by affecting miRNA and siRNA (Yin et al. 2019). Another fungal effector, VdSSR1, secreted by *V. dahliae*, suppresses AGO1-miRNA complex nuclear export by chelating ALY family proteins, thereby reducing miRNA accumulation and cross-kingdom silencing (Zhu et al. 2022).

Tudor-SN (TSN) is a component of the RISC; it contains nuclease domains and plays a critical role in the RNAi mechanism (Caudy et al. 2003). TSN is composed of four conserved SN domains and one TSN composite domain, and is conserved across eukaryotes (Sundstrom et al. 2009). Studies in mammals have revealed the multifunctional nature of TSN, as it participates in transcriptional regulation, pre-mRNA splicing, post-transcriptional regulation and the degradation of modified pri-miRNAs (Cui et al. 2018; Zhang et al. 2023; Elbarbary et al. 2017; Yang et al. 2006; Cappellari et al. 2014). Additionally, research in plants and animals has shown that TSN affects the assembly rate of the formation of stress granules and P-bodies, contributing to mRNA stabilisation (Su et al. 2017; Gutierrez-Beltran, Bozhkov, et al. 2015; Gutierrez-Beltran, Moschou, et al. 2015). Although TSN is one of the earliest identified RISC protein members, its precise function within the RNAi mechanism remains largely unexplored.

In this study, we report the identification of an effector in *V. mali* that exhibits RNA silencing suppressor activity. VmSR1 interferes with RNA silencing by accelerating the degradation of TSN2 protein, subsequently leading to a significant decrease in miRNA abundance and plant disease resistance.

2 | Results

2.1 | VmSR1 Is Required for the Virulence of *V. mali*

In our previous analysis of the *V. mali* genome, we identified 774 secreted proteins (Yin et al. 2015). Through testing their ability to suppress BAX-induced cell death, several effectors were discovered, including VmPR1c and VmEP1 (Li et al. 2015; Han et al. 2024; Wang, Wang, et al. 2022). We identified another effector, VmSR1, which was also found to inhibit BAX- and INF1-induced cell death (Figure 1a). To investigate whether VmSR1 is involved in the pathogenicity of *V. mali*, we examined the expression of *VmSR1* in the wild-type (WT) strain during the infection of apple branches. The results showed that *VmSR1* expression was upregulated during the early stages of infection (Figure S1). *VmSR1* encodes a 553-amino acid (aa) protein. Protein sequence analysis revealed that the N-terminal 20 aa of VmSR1 constitute a signal peptide, and its secretion function was verified using a yeast secretion capability validation (Figure 1b). To investigate the localisation of VmSR1 in the infected tissues, we constructed an overexpression vector MgRP27:*VmSR1-GFP* and transformed it into *V. mali*, generating *VmSR1-GFP* overexpression strains (Figure S2a). The overexpression strains and the WT *V. mali* were used to inoculate apple leaves. Leaf tissues were collected from the boundary region between the lesion and healthy areas for microscopic observation (Figure S2b). Microscopy analysis revealed that cells infected by the *VmSR1-GFP* strain exhibited markedly stronger GFP fluorescence signals compared to those infected by the WT strain, and many condensates were observed in multiple cells. In contrast, cells infected with the WT strain only exhibited weak fluorescence, with no visible condensates within the cells (Figure S2c). These results suggest that VmSR1 is present in infected tissues.

To determine the effect on pathogenicity by VmSR1, two *VmSR1* knockout mutants were generated via polyethylene glycol (PEG)-mediated protoplast transformation (Figure S3a). Pathogenicity tests on apple branches revealed that the *VmSR1* mutants exhibited significantly reduced virulence compared to the WT strain (Figure 1c). No significant effect on mycelial vegetative growth was observed when the two knockout mutants and the WT strain were cultured on potato dextrose agar (PDA) plates (Figure S3b). After complementing the *VmSR1* gene in the mutant strain, the pathogenicity on apple twigs was restored, similar to that of the WT *V. mali* (Figure 1d, Figure S3c). These results indicate that VmSR1, as an effector, plays an important role in the pathogenesis of *V. mali*.

2.2 | VmSR1 Suppresses Plant Immunity

Transient overexpression of *GFP* or *VmSR1* in apple leaves and subsequently inoculating the WT *V. mali* strain showed that overexpression of *VmSR1* enhanced the pathogenicity of the WT strain, as indicated by a significant increase in mycelial biomass (Figure 2a,b). Several defence-related genes in the salicylic acid (SA) signalling pathway were downregulated after overexpressing *VmSR1* (Figure S4). Staining for reactive oxygen species (ROS) and callose in these leaves demonstrated that the levels of ROS and callose were significantly lower in *VmSR1*-overexpressing leaves compared to the control (Figure 2c,d). These findings imply that *VmSR1*, a critical virulence factor of *V. mali*, enhances the pathogen's virulence by modulating the plant's immune response.

2.3 | VmSR1 Interacts With NbTSN2 and MdTSN2

To elucidate the mechanism by which VmSR1 functions as an effector in plants, co-immunoprecipitation-mass spectrometry

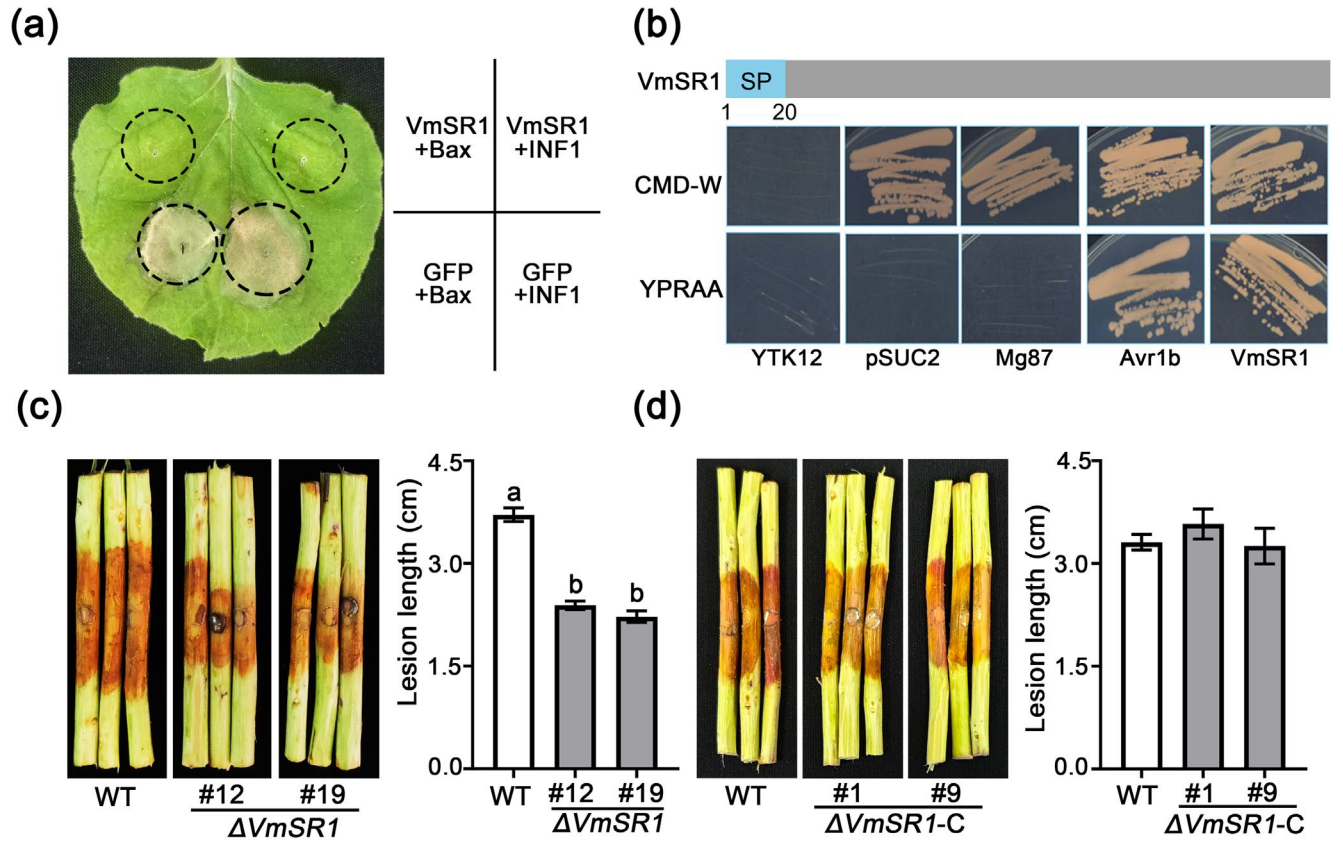

FIGURE 1 | VmSR1 is a virulence effector in *Valsa mali*. (a) VmSR1 transiently expressed effectively inhibits BAX- and INF1-triggered cell death in *Nicotiana benthamiana*. (b) Signal peptide analysis and secretory function verification of VmSR1. The pSUC2 empty plasmid and the non-secreted protein Mg87 from *Magnaporthe oryzae* were used as the negative controls, while Avr1b from *Phytophthora sojae* was used as the positive control. (c) *VmSR1* deletion mutants (#12 and #19) showed reduced virulence in apple twigs compared to the wild type (WT). The length of lesions after inoculation was measured at 3 days post-inoculation (dpi). Values are mean ± SE ($n \geq 8$). Different lowercase letters denote significant differences, Duncan's test, $\alpha = 0.05$. (d) *VmSR1* mutant complemented strains (#1 and #9) recovered virulence in apple twigs. The length of lesions after inoculation was measured at 3 dpi. Values are mean ± SE ($n \geq 8$), Student's *t* test.

(Co-IP-MS) was used to analyse the proteins that VmSR1 interacts with in *Nicotiana benthamiana* (Table S1). Among the identified candidates, the TSN2 protein, a homologous protein previously known as a component of the RISC in *Caenorhabditis elegans*, *Drosophila* and mammals, was identified as a potential interactor of VmSR1. The TSN protein is highly conserved across eukaryotes and is structurally characterised by four tandemly arranged SNc domains and a Tudor-SNc fusion domain (Figure S5a,b).

Using TaWPI6-mCherry (a plasma membrane marker) as a control, we observed that MdTSN2 and NbTSN2 localised in the cytoplasm (Figure S6a). When VmSR1-GFP was co-expressed with MdTSN2-mCherry or NbTSN2-mCherry, the observation of fluorescence and analysis of fluorescence signals showed that VmSR1 colocalised with MdTSN2 or NbTSN2 (Figure S6b,c). These results were further validated through bimolecular fluorescence complementation (BiFC) assays, which confirmed the interaction between VmSR1 and TSN2 proteins, with condensates forming in the cytoplasm (Figure 3a). To investigate the domains of MdTSN2 or NbTSN2 interacting with VmSR1, we generated a series of truncated TSN variants based on the domain characteristics of TSN2 and performed BiFC experiments (Figure 3a, Figure S7). The results showed that the three SNc domains at the N-terminus of TSN are essential for its binding to VmSR1.

Additionally, Co-IP assays in *N. benthamiana* leaves co-expressing VmSR1-GFP with either MdTSN2-FLAG or NbTSN2-FLAG validated their interaction in vivo (Figure 3b). Luciferase complementation imaging assays showed a strong luciferase signal in leaves co-infiltrated with VmSR1 and MdTSN2 or NbTSN2 (Figure 3c).

2.4 | VmSR1 Promotes Degradation of TSN Proteins

In order to explore the changes of TSN2 caused by VmSR1 binding, we expressed both in *N. benthamiana* simultaneously and observed that VmSR1 caused a modest reduction in TSN2 protein levels (Figure 4a,b). Following CHX treatment, the degradation rate of TSN2 proteins increased. However, the degradation of TSN2 proteins was suppressed by the proteasome inhibitor MG132, indicating that the proteasome degradation pathway is involved in VmSR1-induced TSN2 protein turnover

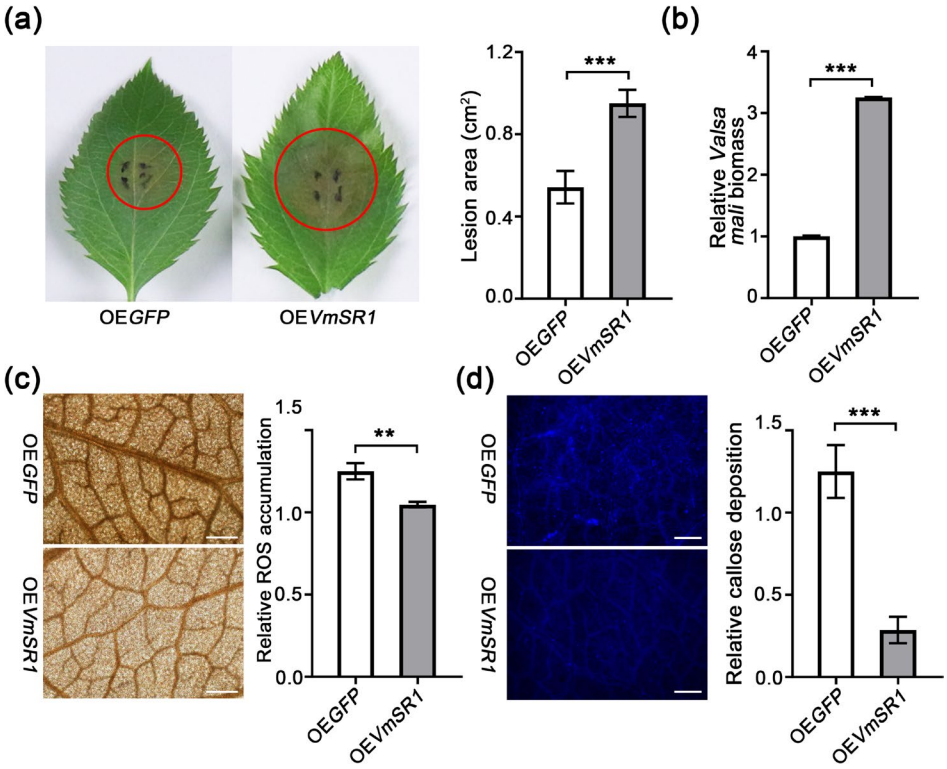

FIGURE 2 | VmSR1 inhibits plant immune responses. (a) Overexpression of *VmSR1* reduced apple resistance to *Valsa mali*. *V. mali* wild-type was inoculated on apple leaves at 4 days post-agro-infiltration. Photographs were taken at 36 h post-inoculation (hpi). Lesion areas were measured using ImageJ software. Values are mean ± SE ($n \geq 12$). (b) Relative fungal biomass analysis. (c) The accumulation of reactive oxygen species (ROS) in apple leaves transiently overexpressing *GFP* or *VmSR1* at 72 hpi. Bar, 50 μm. (d) The callose deposition in apple leaves transiently overexpressing *GFP* or *VmSR1* at 72 hpi. Bar, 50 μm. ImageJ software was used to quantify callose deposition and ROS accumulation per microscopic picture. $^{**}p < 0.01$, $^{***}p < 0.001$, Student's *t* test.

(Figure 4a,b). In the cell-free degradation assay, exogenously added MdTSN2 or NbTSN2 proteins, purified through prokaryotic expression systems, degraded more rapidly in protein extracts prepared from *VmSR1*-overexpressing *N. benthamiana* leaves compared to extracts from *GFP*-overexpressing control leaves (Figure 4c,d). These results strongly suggest that VmSR1 facilitates the degradation of TSN2 proteins, probably by altering the stability of these proteins in planta.

2.5 | VmSR1 Suppresses RNA Silencing

TSN is a component of the RISC complex in mammals. We hypothesised that VmSR1, which interacts with TSN, might function as an RNA silencing suppressor in plants. The 16c *N. benthamiana* line, which stably expresses GFP, is commonly used for RNA silencing studies. When GFP is re-expressed in 16c *N. benthamiana*, it triggers RNA silencing, resulting in silencing of fluorescence in the injected area. Analogous to the known RNA silencing suppressors PSR1 and P19, VmSR1 inhibited RNA silencing-mediated GFP fluorescence loss in 16c *N. benthamiana* (Figure 5a). Reverse transcription-quantitative PCR (RT-qPCR) analysis further demonstrated that *VmSR1* overexpression led to a significant increase in GFP mRNA compared to the control, which co-infiltrated GFP with an empty vector (Figure 5b). Consistently, GFP content in the *VmSR1* overexpression group was markedly elevated relative to the control, corroborating the fluorescence observations (Figure 5c). These findings suggest that VmSR1 inhibited the RNA silencing process in 16c *N. benthamiana*.

2.6 | VmSR1 Inhibits the Abundance of miRNAs in Plants

To investigate the impact of VmSR1 on plant sRNA, we measured the levels of several miRNAs after overexpression of *VmSR1* in apple leaves and *N. benthamiana*. RT-qPCR analysis showed significantly reduced levels of multiple miRNAs (Figure 6a,b). To confirm this phenotype, we generated three independent *Arabidopsis* transgenic lines expressing *VmSR1* and an empty vector control (VC) line via *Agrobacterium*-mediated transformation (Figure S8a). Unlike the growth inhibition caused by overexpression of *PSR1* in *Arabidopsis*, we did not observe significant morphological differences in OE*VmSR1* lines (Figure S8b). We also found that VmSR1 interacted with AtTSN2 (Figure S9). Among the transformed lines, we selected the line with the highest *VmSR1* expression (Line #4) alongside the VC for sRNA (sRNA) library construction and high-throughput sequencing.

After filtering low-quality and irrelevant sequences and normalising the data, we observed that overexpression of *VmSR1* in *Arabidopsis* led to changes in the proportion of 20–25 nucleotide miRNAs, though no significant differences were found when compared to the empty vector-transformed control lines

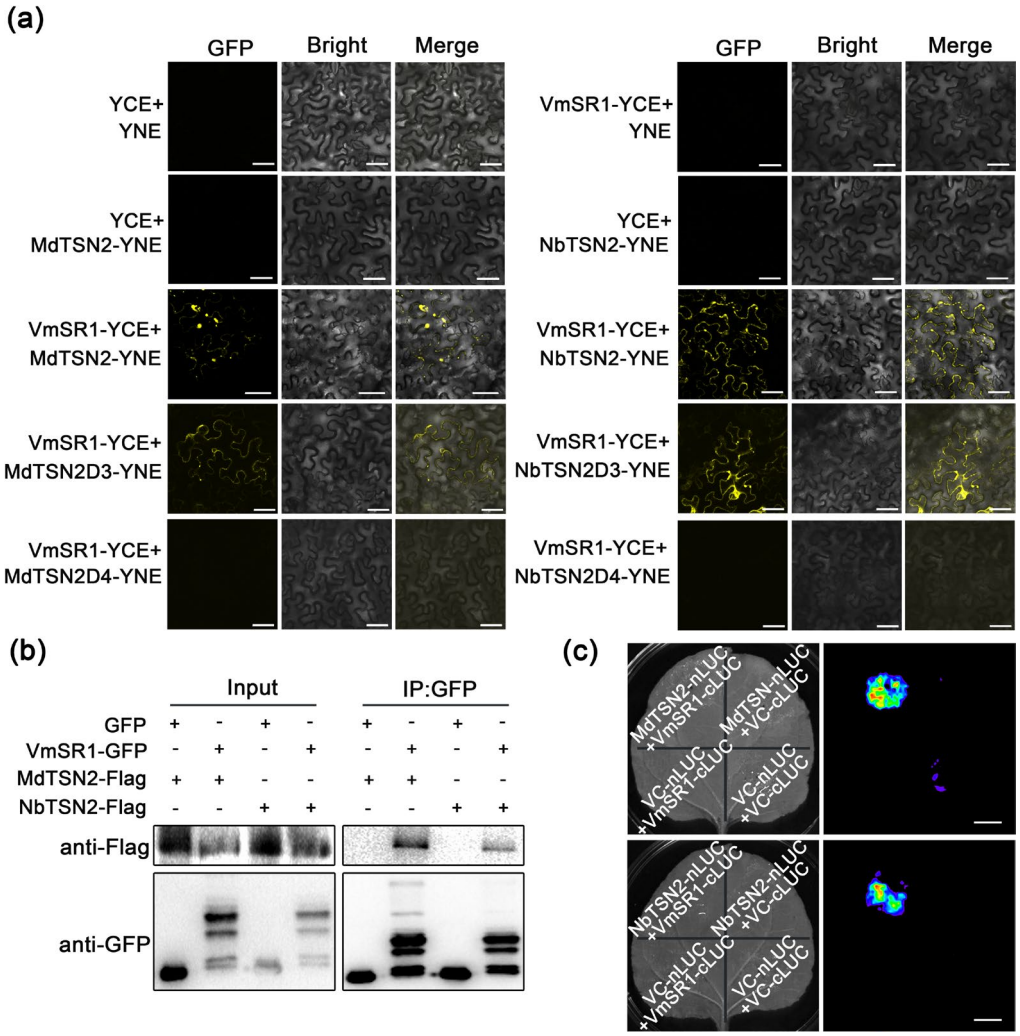

FIGURE 3 | VmSR1 interacts with NbTSN2 or MdTSN2. (a) VmSR1 fused C-YFP (YCE-VmSR1) co-expressed with MdTSN2 or NbTSN2 fused N-YFP (YNE-MdTSN2 or YNE-NbTSN2) in *Nicotiana benthamiana*, and fluorescence was observed after 36 h of agro-infiltration and by laser-scanning confocal microscopy. The transient transformation of YCE-VC and YNE-VC was used as a control. Bar, 50 μm. (b) Co-expression of GFP-tagged VmSR1 and FLAG-tagged MdTSN2 or NbTSN2 in *N. benthamiana* leaves, and co-immunoprecipitation was performed with anti-GFP magnetic beads. Protein samples were subjected to western blotting using anti-GFP and anti-FLAG antibodies. (c) The split-luciferse assay. Co-expression of VmSR1-cLuc and MdTSN2-nLuc or NbTSN2-nLuc in *N. benthamiana* leaves for 48 h and cLUC/nLUC were used as negative controls. Luciferase complementation imaging (LCI) images were captured using a cooled charge-coupled device (CCD) imaging apparatus. Bar, 1 cm.

(Figure S10). However, when we analysed the expression patterns of miRNAs, we found that in the OE*VmSR1 Arabidopsis* line, the expression of 30 miRNAs was significantly downregulated. In contrast, only one miRNA showed significant upregulation (Figure 6c,d). A similar trend was observed in all detected miRNA data; most miRNAs were inhibited in the OE*VmSR1* line (Table S2). To validate the sRNA-sequence data, we measured the abundance of 13 miRNAs in three *VmSR1* overexpression lines and found that their abundance was significantly repressed in *VmSR1*-overexpression lines compared to the VC line (Figure 6e). miRNAs exert their function by promoting mRNA degradation or inhibiting mRNA translation. Therefore, we assessed the mRNA levels of target genes of miR156a, miR158a, miR159b and miR391. In three *VmSR1*-overexpression lines, the mRNA levels of the target genes of these miRNAs were significantly increased (Figure S11). These results indicate that VmSR1 plays a repressive role in regulating plant miRNA abundance.

2.7 | TSN2 Regulates Plant miRNA Content and Disease Resistance

To assess TSN2 function, we silenced *MdTSN2* in apple leaves and assessed miRNA content, which was reduced when *VmSR1* was overexpressed. The results showed that with the decrease in *TSN2* expression, the abundance of these miRNAs also decreased (Figure 7a). The same experiment was performed in *N. benthamiana*, and similar results were observed (Figure 7b). These results suggest that VmSR1 exerts its function of suppressing miRNA abundance by promoting the degradation of the TSN2 protein.

Silencing of *TSN2* in both apple and *N. benthamiana* leaves resulted in a decrease in miRNA abundance. To further investigate its potential involvement in plant immune responses, we performed infection assays. In apple leaves, silencing of *MdTSN2* followed by inoculation with *V. mali* led to a

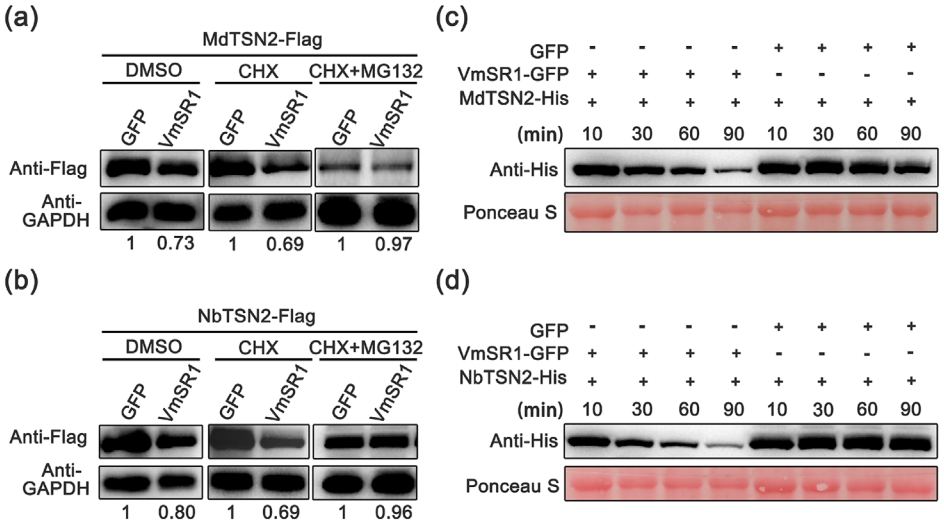

FIGURE 4 | VmSR1 caused degradation of TSN2 protein. (a) VmSR1 promotes MdTSN2 degradation dependent on the proteasome degradation pathway. GAPDH was used as a loading control. (b) VmSR1 promotes NbTSN2 degradation dependent on the proteasome degradation pathway. GAPDH was used as a loading control. (c) Cell-free degradation of His-tagged MdTSN2 proteins. Protein extracts were prepared from *Nicotiana benthamiana* leaves transiently expressing VmSR1 fused GFP (VmSR1-GFP) or GFP. (d) Cell-free degradation of His-tagged NbTSN2 proteins. Protein extracts were prepared from *N. benthamiana* leaves transiently expressing VmSR1 fused GFP (VmSR1-GFP) or GFP.

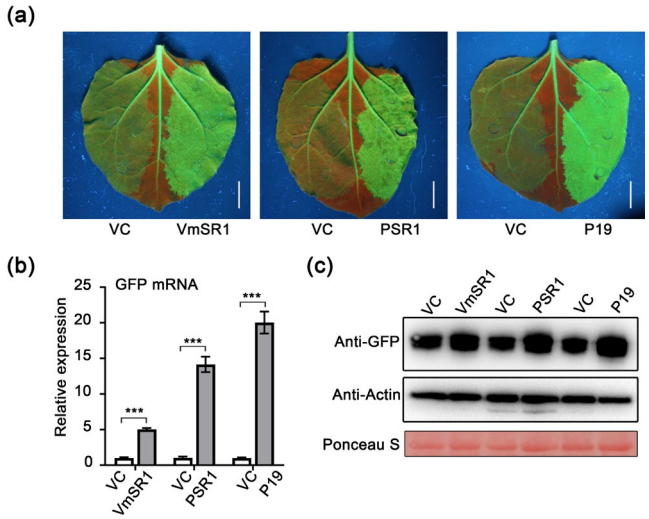

FIGURE 5 | VmSR1 suppressed transgene-mediated GFP silencing in *Nicotiana benthamiana*. (a) RNA silencing suppression in *N. benthamiana* 16c co-infiltrated with *Agrobacterium* delivering GFP with VmSR1, PSR1 or P19. The empty vector pCHF3 was used as a negative control. Pictures were taken 4 days post-infiltration (dpi). Bar, 1 cm (b) GFP mRNA expression levels in the infiltrated *N. benthamiana* 16c leaves were measured by reverse transcripiton-quantitative PCR. The *Actin* gene of *N. benthamiana* was used as an RNA expression reference. ***$p < 0.001$, Student's *t* test. (c) The levels of GFP protein in *N. benthamiana* 16c after 4 days *Agrobacterium* infiltration was detected by western blot. Actin and RuBisCO were used as loading controls.

significant reduction in disease resistance, as evidenced by the increased lesion area (Figure 7c,d). Similarly, silencing of *NbTSN2* in *N. benthamiana* leaves followed by infection with *Sclerotinia. sclerotiorum* displayed a phenotype consistent with that observed in apple leaves, with a significant reduction in resistance to the pathogen (Figure 7e,f). These results suggest that TSN2 plays a crucial role in regulating plant immune responses.

3 | Discussion

Pathogen effector proteins are highly diverse, with their mechanisms of action primarily classified into two categories: suppressing plant disease resistance or enhancing plant susceptibility. For example, the rice fungus *Magnaporthe oryzae* effector MoChia1 targets and regulates the rice immune positive regulator TPR (Tetratricopeptide repeat) protein, while the wheat *Puccinia striiformis* f. sp. *tritici* effector PsSpg1 interacts with the wheat susceptibility protein TaPsIPK1, promoting its nuclear translocation and the phosphorylation of the transcription factor TaCBF1, ultimately facilitating disease progression in wheat (Yang et al. 2019; Wang, Tang, et al. 2022). Unlike the above effectors that directly target plant resistance or disease-susceptibility proteins, pathogens also produce RNA silencing suppressors, a class of effectors less studied in fungi and oomycetes but widely reported in viruses, which function by interfering with plant RNA silencing. Our research shows that VmSR1, an essential effector for the pathogenicity of *V. mali* (Figure 1), suppresses the abundance of multiple miRNAs in apple leaves (Figure 6), ultimately promoting *V. mali* infection (Figure 2). This study provides new evidence and insights into how fungal RNA silencing suppressors contribute to pathogen virulence.

The RNA silencing pathway requires the participation of various proteins and sRNAs, allowing RNA silencing suppressors to perform their respective inhibitory functions through different mechanisms. The P19 protein, which has been widely studied, can bind to the siRNA double strands with high affinity, sequestering them and preventing the assembly of the RISC complex (Silhavy et al. 2002; Vargason et al. 2003). HC-Pro from tobacco etch virus recognises and binds the 3′ overhangs of siRNAs, preventing their assembly into the RISC complex

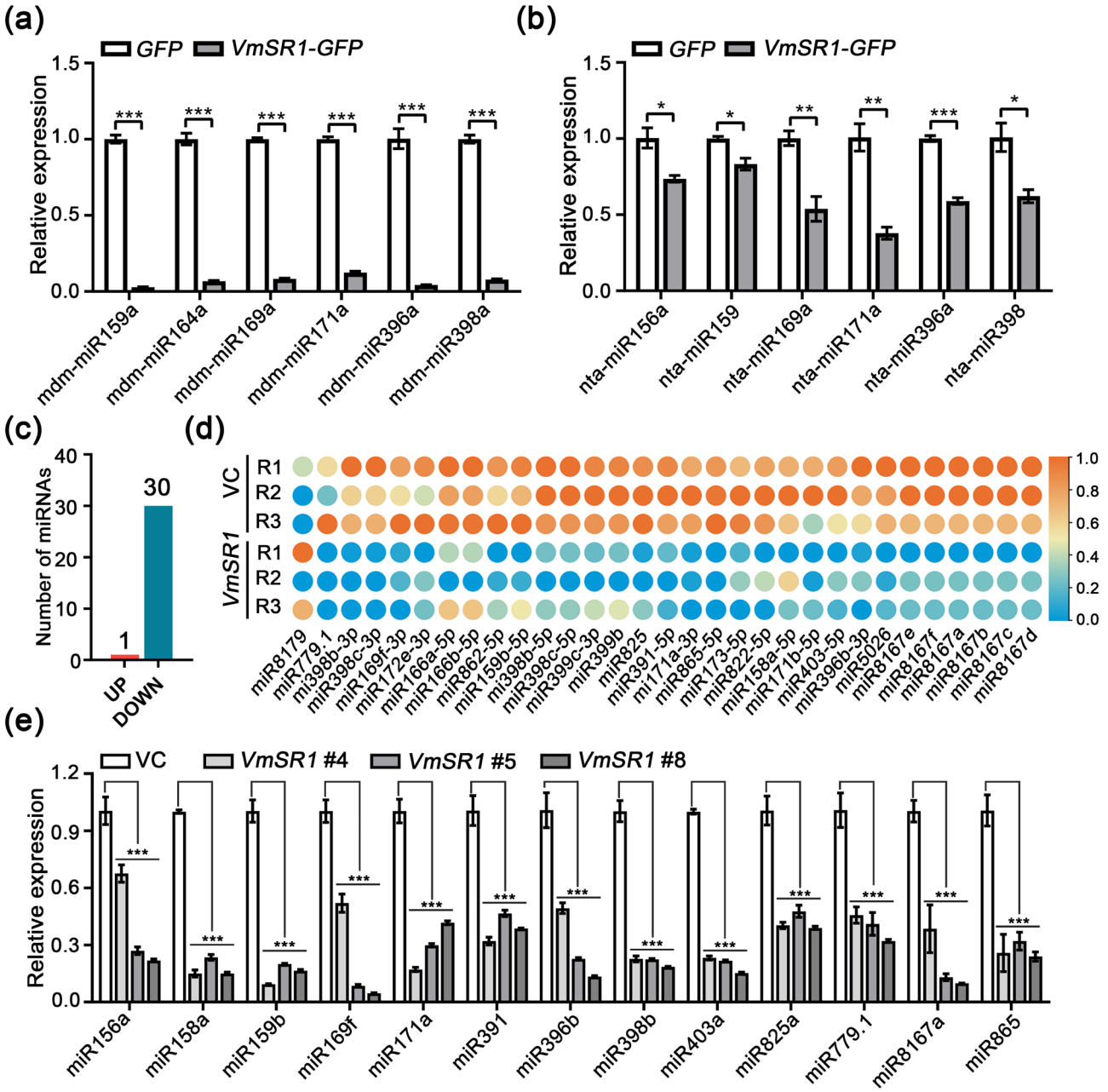

FIGURE 6 | Effects of VmSR1 on miRNAs in plants. (a) Overexpression of *VmSR1* reduced miRNA abundance in apple leaves. (b) Overexpression of *VmSR1* reduced miRNA abundance in *Nicotiana benthamiana*. (c) Statistics of the number of miRNAs with significant changes among empty vector control (VC) versus *VmSR1*. (d) Differential expression heatmap of significant changes in miRNAs in VC and *VmSR1*. VC: Transgenic *Arabidopsis* line transformed with the pCHF3 empty vector; *VmSR1*: Overexpression of *VmSR1* in *Arabidopsis*. R1/R2/R3: Three biological replicates. (e) The relative abundance of miRNAs in *VmSR1* transgenic *Arabidopsis* and VC lines. U6 was used as an RNA expression reference. $^{*}p < 0.05$, $^{**}p < 0.01$, $^{***}p < 0.001$, Student's *t* test.

(Lakatos et al. 2006). The 2b protein produced by cucumber mosaic virus has the ability to directly bind AGO1 and AGO4 of *Arabidopsis* and inhibit their slicing enzyme activity (Gonzalez et al. 2010; Zhang et al. 2006). Unlike viral RNA silencing suppressors, which usually exert their effects by directly binding to sRNA or targeting AGO proteins, the mechanisms of RNA silencing suppressors identified in fungi and oomycetes are more complex. PSR1 from *P. sojae* inhibits sRNA biosynthesis and RNA metabolism by reducing the RNA helicase activity, RNA and pri-miRNA binding activity of its target protein PINP1 (Qiao et al. 2015; Gui et al. 2022; Zhang et al. 2019). VdSSR1, secreted by *V. dahliae*, binds to ALY family proteins in the plant nucleus, interfering with the nuclear export of the AGO1-miRNA complex and leading to a significant decrease in the levels of cytoplasmic AGO1 protein and sRNA (Zhu et al. 2022). This study found that VmSR1 secreted by *V. mali* reduced the abundance of multiple miRNAs in apple leaves, *Arabidopsis* and *N. benthamiana* (Figure 6). We showed that VmSR1 accelerated the degradation of plant Tudor-SN2 proteins, thereby altering sRNA abundance (Figure 7). After comparing the protein sequence of VmSR1 with the RNA silencing suppressors reported in *P. sojae*, *P. striiformis* f. sp. *tritici* and *V. dahliae*, no homologous

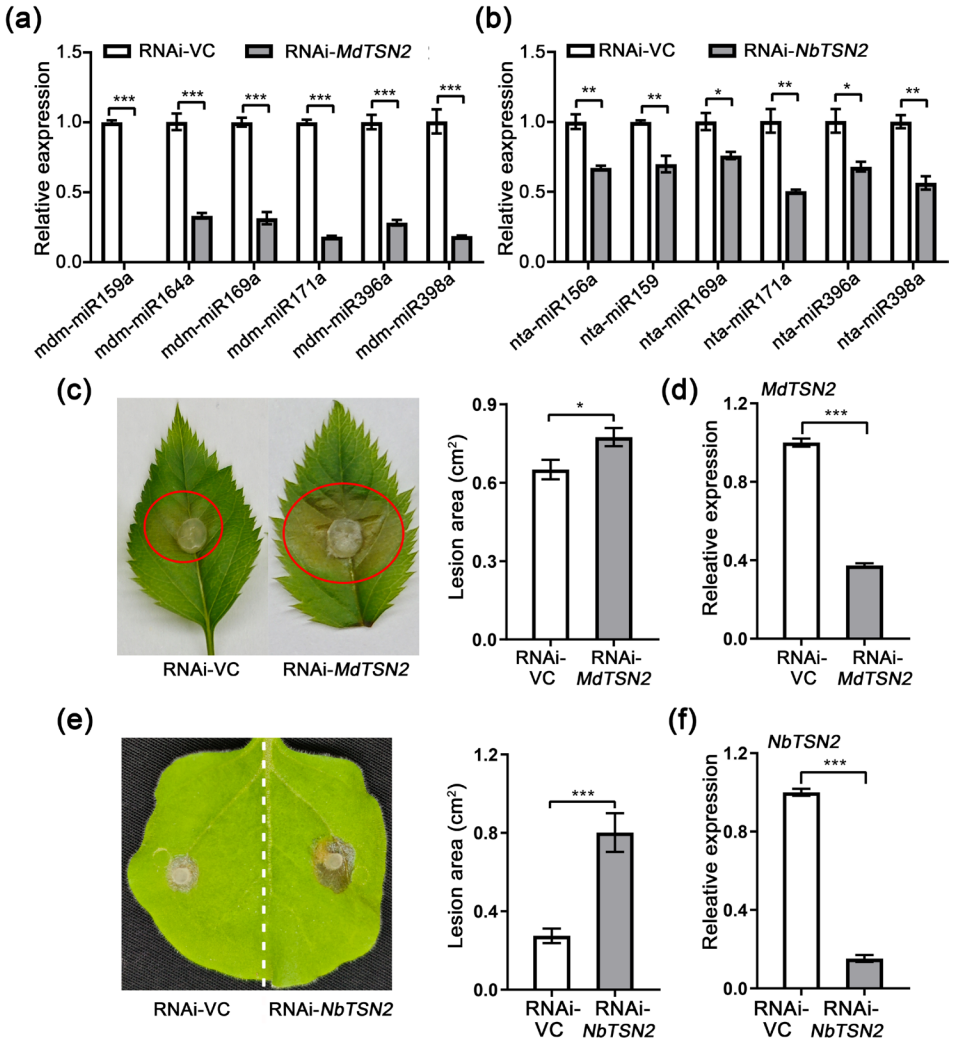

FIGURE 7 | Silencing of *TSN2* suppressed miRNA levels and reduced plant disease resistance. (a) The content of multiple miRNAs in apple leaves, in which *MdTSN2* was silenced, was measured by reverse transcription-quantitative PCR (RT-qPCR). *MdU6* was used as an internal reference. VC, empty vector control. (b) The content of multiple miRNAs in *Nicotiana benthamiana* leaves, in which *NbTSN2* was silenced, was measured by RT-qPCR. *NbU6* was used as an internal reference. (c) Silencing of *MdTSN2* reduced apple resistance to *Valsa mali*. *V. mali* was inoculated on apple leaves at 4 days post-agro-infiltration. Photographs were taken at 36 h post-infiltration (hpi). Lesion areas were measured using ImageJ. Values are mean ± SE ($n \geq 33$). (d) Identification of the expression of *MdTSN2* after RNA silencing. (e) Silencing of *NbTSN2* reduced resistance to *Sclerotinia sclerotiorum*. *S. sclerotiorum* was inoculated on *N. benthamiana* leaves at 48 h post agro-infiltration. Photographs were taken at 24 hpi. Lesion areas were measured using ImageJ. Values are mean ± SE ($n = 12$). (f) Identification of the expression of *NbTSN2* after RNA silencing. $^{*}p < 0.05$, $^{**}p < 0.01$, $^{***}p < 0.001$, Student's *t* test.

sequences or conserved structures were identified (Figure S12). This suggests that the generation of RNA silencing suppressors in different pathogens is likely independent, rather than resulting from early genetic variation and inheritance.

The TSN protein is conserved in plants and animals and has a structure consisting of four repeated staphylococcal nuclease-like (SNc) domains at the N-terminus and a C-terminal SNc5a-Tudor-SNc5b (TSN) domain (Li et al. 2008). The staphylococcal nuclease domain confers nuclease activity to the TSN proteins, which can bind to and cleave RNA molecules (Caudy et al. 2003). Crystal structure analysis showed that the SNc3 and SNc4 domains of the TSN protein can bind to dsRNA (Li et al. 2008). Deletion of the SNc1 or SNc4 domain causes TSN to lose its ability to bind to miR-31-5P (Elbarbary et al. 2017). Our results showed that the interaction between VmSR1 and TSN2 depends on the SNc1 to SNc3 domains of TSN2, and the absence of this structure prevented the interaction (Figure 3, Figure S7). We speculate that VmSR1 binding to the SNc1 to SNc3 regions of TSN2 prevents TSN2 from binding to sRNA.

We found that silencing of *TSN2* in *N. benthamiana* and apple leaves resulted in reduced levels of multiple miRNAs (Figure 7). The knockout of *TSN* in HeLa cells results in upregulation of a cohort of miRNAs that inhibit the G1 to S phase transition, but also downregulate the expression of many other miRNAs (Elbarbary et al. 2017). Loss of *TSN* led to diametrically opposed changes in the levels of different miRNAs, indicating that TSN has a multifaceted regulatory effect on miRNA abundance. Subsequent studies should attempt to identify the similarities

and differences of these differentially altered miRNAs to gain insight into the role of TSN in RNA silencing.

In conclusion, our study identified a key virulence effector, VmSR1, from *V. mali* that functions as an RNA silencing suppressor in the pathogen's infection strategy. We further explored the interaction between VmSR1 and TSN2 and found that VmSR1 promotes TSN2 degradation, leading to reduced miRNA abundance and subsequent weakening of plant disease resistance. These findings deepen our understanding of fungal pathogenesis and open new avenues for advancing plant disease resistance research.

4 | Experimental Procedures

4.1 | Strains, Plant Materials and Growth Conditions

The WT strain of *V. mali* 03-8 was stored in the Research Team of Pathogen Biology and Integrated Control of Fruit Trees at the College of Plant Protection, Northwest A&F University, China. All strains were cultured in PDA at 25°C in the dark. *Escherichia coli* DH5 was cultured in Luria Bertani (LB) medium at 37°C. *Agrobacterium tumefaciens* GV3101 was cultured on yesat extract peptone (YEP) medium at 28°C.

Nicotiana benthamiana, including WT and a GFP-expressing transgenic line (16c) (Ruiz et al. 1998), was cultivated at 25°C. *A. thaliana* ecotype Columbia (Col-0) and transgenic lines were cultivated at 21°C. Apple (*M. domestica* 'GL-3') tissue culture plants were grown on Murashige and Skoog (MS) medium in a glasshouse at 22°C. All plants were grown under a 16 h:8 h light/dark cycle. Apple twigs (*M. domestica* 'Fuji') were obtained from the experimental orchard at Northwest A&F University.

4.2 | Gene Knock-Out, Complementation in *V. mali*

Gene knock-out and complementation were performed as previously described (Xu et al. 2020). The *VmSR1* gene knockout fragment was obtained by double-joint PCR, and PEG-mediated protoplast transformation was used to obtain transformants (Gao et al. 2011). Transformants were selected on a PDA plate containing 120 μg/mL hygromycin. DNA was extracted by the alkaline lysis method and detected by PCR with the primers in Table S3. Using pFL2-VmSR1-F and pFL2-VmSR1-R as primers amplifies the complemented fragments and connects the pFL2 vector to obtain recombinant plasmids to transform protoplasts. The transformants were picked for PCR.

4.3 | Virulence Tests of *V. mali*

Apple twigs of cv. Fuji and leaves of GL-3 were used for the virulence tests. *V. mali* WT strain 03-8 and *VmSR1* knockout mutants were cultured on PDA plate for 2 days. Mycelial plugs (5 mm diameter) were inoculated on the apple twigs at room temperature with high humidity and lesion length was measured after 3 days.

4.4 | Bioinformatics Analysis

The nucleic acid sequence and protein sequence were obtained from the NCBI database (https://www.ncbi.nlm.nih.gov/) according to respective gene ID: *VmSR1* Vm1G-07201; *NbTSN2* LOC107815454; *MdTSN2* LOC103438667. The VmSR1 protein signal peptide was predicted using the SignalP 6.0 server (http://www.cbs.dtu.dk/services/SignalP/). MEGA 7 was used to build phylogenetic dendrograms with maximum likelihood.

4.5 | BiFC Assays

The coding sequences for *VmSR1* and *NbTSN2* or *MdTSN2* were cloned into the BiFC vectors 35S-SPYCE(M) and 35S-SPYNE(R), respectively, and transformed into *A. tumefaciens*. The VmSR1-YCE was transiently co-expressed in *N. benthamiana* leaves together with TSN2-YNE using *A. tumefaciens* GV3101-mediated infiltration (Han et al. 2024). The YFP fluorescence signal was observed after 48 h with an FV3000 laser-scanning confocal microscope (Olympus).

4.6 | Co-IP Assays

The coding sequences for *VmSR1* and *NbTSN2* or *MdTSN2* were cloned into pCAMBIA1302-eGFP and pCAMBIA1302-FLAG vectors. The pCAMBIA1302-eGFP plasmid served as a negative control. The TSN2-FLAG was transiently co-expressed in *N. benthamiana* leaves together with VmSR1-eGFP or eGFP using *A. tumefaciens* GV3101-mediated infiltration (Wang et al. 2021). Total proteins were extracted using an extraction buffer (1 M Tris–HCl pH 7.5, 5 M NaCl, 0.5 M EDTA, 20% glycerol, 10 mM dithiothreitol, 0.1% protease inhibitor, 1 mM PMSF), and then incubated with anti-GFP magnetic beads for 2 h with gentle shaking. The beads were washed five times with washing buffer according to the manufacturer's manuals after incubation and resuspended with 40 μL phosphate-buffered saline (PBS) for the preparation of protein samples. Co-precipitation signal was determined by immunoblotting using an anti-FLAG or anti-GFP antibody.

4.7 | RNA Silencing Suppression Assay

RNA silencing suppression assays were performed on the six-leaf stage *N. benthamiana* 16c plants as previously described (Qiao et al. 2013; Yin et al. 2019). The second and third fully expanded leaves were co-infiltrated with *Agrobacterium* strains carrying pCAMBIA1302-35S:GFP and individual effector gene constructs. *Agrobacterium* carrying viral P19 and oomycete PSR1 were used as positive controls. The empty vector pCHF3 (with no genes inserted) was used as a negative control. Experiments were repeated at least three times. Green fluorescence was visualised using a long-wavelength UV lamp (Blak-Ray B-100AP, Ultraviolet Products), and leaves were photographed at 4 days post-infiltration.

4.8 | sRNA Analysis in *Arabidopsis* Transgenic Lines Overexpressing *VmSR1*

Arabidopsis thaliana Col-0 plants were transformed with *A. tumefaciens* GV3101 carrying pCHF3 VC or pCHF3-*VmSR1* by the floral-dip method. Three independent lines were analysed for *VmSR1* expression by RT-qPCR. Leaves of the *VmSR1* transgenic line (Line #4) with the highest expression and the empty VC line were collected for sRNA-seq (Gene Denovo; Guangzhou, China).

4.9 | sRNA Sequencing

Total RNA was extracted from the leaves of *Arabidopsis* transgenic lines. sRNAs with 15–30 nucleotides in size were purified from 200 μg total RNA by denaturing polyacrylamide gel. sRNA libraries were prepared and sequenced using Illumina NovaSeq X Plus by Gene Denovo Biotechnology Co. (Guangzhou, China). The sRNA reads were trimmed for adaptor sequence using Perl scripts and mapped to the *Arabidopsis* genome (The *Arabidopsis* Information Resource 9.0, for microRNA [miRNA] abundance) or miRNA hairpin sequences (from miRBase version 1.8, for miRNA imprecision).

4.10 | RNA Extraction, cDNA Synthesis and qPCR Analysis

Polysaccharide Polyphenol Plant Total RNA Extraction Kit (Tiangen) was used to extract total RNAs from samples. Reverse transcription was conducted using oligo(dT) primers from the Revert Aid First-strand cDNA Synthesis Kit (Thermo Scientific) according to the manufacturer's guidelines. For sRNA expression detection, sRNAs were extracted with SanPrep Column microRNA Extraction Kit (Sangon Biotech), and cDNA was synthesised using Mir-X miRNA First-Strand Synthesis Kit (Takara). qPCR was performed in triplicate on a CFX96 Touch Real-Time PCR Detection System (Bio-Rad) apparatus with 2×RealStar Fast SYBR qPCR Mix (GenStar). Fold-changes in gene expression were calculated using the $2^{-\Delta\Delta Ct}$ method, and *Actin* or *U6* was used as the endogenous control.

4.11 | Statistical Analysis

The data were analysed using GraphPad Prism (GraphPad Software) and presented as means ± SE. All assays were performed in triplicate.

Acknowledgements

The authors thank Professor Yi Li at Peking University for providing the *N. benthamiana* 16c. This work was financially supported by the Special Support Plan for High-level Talent of Shaanxi Province (to L.H., grant F1020221012) and the Major Scientific and Technological Special Projects of Shaanxi Province (2020ZDZX03-03-01).

Conflicts of Interest

The authors declare no conflicts of interest.

Data Availability Statement

The data that support the findings of this study are available from the corresponding author upon reasonable request.

References

Anandalakshmi, R., G. J. Pruss, X. Ge, et al. 1998. "A Viral Suppressor of Gene Silencing in Plants." *Proceedings of the National Academy of Sciences of the United States of America* 95: 13079–13084.

Brigneti, G., O. Voinnet, W. X. Li, L. H. Ji, S. W. Ding, and D. C. Baulcombe. 1998. "Viral Pathogenicity Determinants Are Suppressors of Transgene Silencing in *Nicotiana benthamiana*." *EMBO Journal* 17: 6739–6746.

Cai, Q., L. Qiao, M. Wang, et al. 2018. "Plants Send Small RNAs in Extracellular Vesicles to Fungal Pathogen to Silence Virulence Genes." *Science* 360: 1126–1129.

Cappellari, M., P. Bielli, M. P. Paronetto, et al. 2014. "The Transcriptional Co-Activator SND1 Is a Novel Regulator of Alternative Splicing in Prostate Cancer Cells." *Oncogene* 33: 3794–3802.

Caudy, A. A., R. F. Ketting, S. M. Hammond, et al. 2003. "A Micrococcal Nuclease Homologue in RNAi Effector Complexes." *Nature* 425: 411–414.

Che, R., C. Liu, Q. Wang, et al. 2023. "The *Valsa mali* Effector Vm1G-1794 Protects the Aggregated MdEF-Tu From Autophagic Degradation to Promote Infection in Apple." *Autophagy* 19: 1745–1763.

Cui, X., C. Zhao, X. Yao, et al. 2018. "SND1 Acts as an Anti-Apoptotic Factor via Regulating the Expression of lncRNA UCA1 in Hepatocellular Carcinoma." *RNA Biology* 15: 1364–1375.

Elbarbary, R. A., K. Miyoshi, J. R. Myers, et al. 2017. "Tudor-SN-Mediated Endonucleolytic Decay of Human Cell MicroRNAs Promotes G(1)/S Phase Transition." *Science* 356: 859–862.

Elbashir, S. M., J. Martinez, A. Patkaniowska, W. Lendeckel, and T. Tuschl. 2001. "Functional Anatomy of siRNAs for Mediating Efficient RNAi in *Drosophila melanogaster* Embryo Lysate." *EMBO Journal* 20: 6877–6888.

Feng, H., C. Wang, Y. He, et al. 2023. "Apple Valsa Canker: Insights Into Pathogenesis and Disease Control." *Phytopathology Research* 5: 968432.

Gao, J., Y. Li, X. Ke, Z. Kang, and L. Huang. 2011. "[Development of genetic transformation system of Valsa mali of apple mediated by PEG]." *Wei Sheng Wu Xue Bao* 51: 1194–1199.

Gonzalez, I., L. Martinez, D. V. Rakitina, et al. 2010. "Cucumber Mosaic Virus 2b Protein Subcellular Targets and Interactions: Their Significance to RNA Silencing Suppressor Activity." *Molecular Plant–Microbe Interactions* 23: 294–303.

Gui, X., P. Zhang, D. Wang, et al. 2022. "*Phytophthora* Effector PSR1 Hijacks the Host Pre-mRNA Splicing Machinery to Modulate Small RNA Biogenesis and Plant Immunity." *Plant Cell* 34: 3443–3459.

Gutierrez-Beltran, E., P. N. Moschou, A. P. Smertenko, and P. V. Bozhkov. 2015. "Tudor Staphylococcal Nuclease Links Formation of Stress Granules and Processing Bodies With mRNA Catabolism in *Arabidopsis*." *Plant Cell* 27: 926–943.

Gutierrez-Beltran, E., P. V. Bozhkov, and P. N. Moschou. 2015. "Tudor Staphylococcal Nuclease Plays Two Antagonistic Roles in RNA Metabolism Under Stress." *Plant Signaling & Behavior* 10: e1071005.

Han, P., C. Wang, F. Li, et al. 2024. "*Valsa mali* PR1-Like Protein Modulates an Apple Valine-Glutamine Protein to Suppress JA Signaling-Mediated Immunity." *Plant Physiology* 194: 2755–2770.

He, B., Q. Cai, L. Qiao, et al. 2021. "RNA-Binding Proteins Contribute to Small RNA Loading in Plant Extracellular Vesicles." *Nature Plants* 7: 342–352.

Hou, Y., Y. Zhai, L. Feng, et al. 2019. "A Phytophthora Effector Suppresses Trans-Kingdom RNAi to Promote Disease Susceptibility." *Cell Host & Microbe* 25: 153–165.e155.

Lakatos, L., T. Csorba, V. Pantaleo, et al. 2006. "Small RNA Binding Is a Common Strategy to Suppress RNA Silencing by Several Viral Suppressors." *EMBO Journal* 25: 2768–2780.

Li, C. L., W. Z. Yang, Y. P. Chen, and H. S. Yuan. 2008. "Structural and Functional Insights Into Human Tudor-SN, a Key Component Linking RNA Interference and Editing." *Nucleic Acids Research* 36: 3579–3589.

Li, Z., Z. Yin, Y. Fan, M. Xu, Z. Kang, and L. Huang. 2015. "Candidate Effector Proteins of the Necrotrophic Apple Canker Pathogen *Valsa mali* Can Suppress BAX-Induced PCD." *Frontiers in Plant Science* 6: 579.

Liang, J., J. Wang, K. Wang, H. Feng, and L. Huang. 2024. "VmRDR2 of *Valsa mali* Mediates the Generation of VmR2-siR1 That Suppresses Apple Resistance by RNA Interference." *New Phytologist* 243: 1154–1171.

Mao, Y. B., W. J. Cai, J. W. Wang, et al. 2007. "Silencing a Cotton Bollworm P450 Monooxygenase Gene by Plant-Mediated RNAi Impairs Larval Tolerance of Gossypol." *Nature Biotechnology* 25: 1307–1313.

McManus, M. T., and P. A. Sharp. 2002. "Gene Silencing in Mammals by Small Interfering RNAs." *Nature Reviews Genetics* 3: 737–747.

Melnyk, C. W., A. Molnar, A. Bassett, and D. C. Baulcombe. 2011. "Mobile 24 nt Small RNAs Direct Transcriptional Gene Silencing in the Root Meristems of *Arabidopsis thaliana*." *Current Biology* 21: 1678–1683.

Meng, Y., Y. Xiao, S. Zhu, L. Xu, and L. Huang. 2024. "VmSpm1: A Secretory Protein From *Valsa mali* That Targets Apple's Abscisic Acid Receptor MdPYL4 to Suppress Jasmonic Acid Signaling and Enhance Infection." *New Phytologist* 244: 2489–2504.

Navarro, L., P. Dunoyer, F. Jay, et al. 2006. "A Plant miRNA Contributes to Antibacterial Resistance by Repressing Auxin Signaling." *Science* 312: 436–439.

Qiao, Y. L., L. Liu, Q. Xiong, et al. 2013. "Oomycete Pathogens Encode RNA Silencing Suppressors." *Nature Genetics* 45: 330–333.

Qiao, Y., J. Shi, Y. Zhai, Y. Hou, and W. Ma. 2015. "Phytophthora Effector Targets a Novel Component of Small RNA Pathway in Plants to Promote Infection." *Proceedings of the National Academy of Sciences of the United States of America* 112: 5850–5855.

Qu, F., and T. J. Morris. 2002. "Efficient Infection of *Nicotiana benthamiana* by Tomato Bushy Stunt Virus Is Facilitated by the Coat Protein and Maintained by p19 Through Suppression of Gene Silencing." *Molecular Plant–Microbe Interactions* 15: 193–202.

Ruiz, M. T., O. Voinnet, and D. C. Baulcombe. 1998. "Initiation and maintenance of virus-induced gene silencinb." *Plant Cell* 10: 937–946.

Schnettler, E., H. Hemmes, R. Goldbach, and M. Prins. 2008. "The NS3 Protein of Rice Hoja Blanca Virus Suppresses RNA Silencing in Mammalian Cells." *Journal of General Virology* 89: 336–340.

Silhavy, D., A. Molnar, A. Lucioli, et al. 2002. "A Viral Protein Suppresses RNA Silencing and Binds Silencing-Generated, 21- to 25-Nucleotide Double-Stranded RNAs." *EMBO Journal* 21: 3070–3080.

Su, C., X. Gao, W. Yang, et al. 2017. "Phosphorylation of Tudor-SN, a Novel Substrate of JNK, Is Involved in the Efficient Recruitment of Tudor-SN Into Stress Granules." *Biochimica et Biophysica Acta - Molecular Cell Research* 1864: 562–571.

Sun, Y., D. Luo, Y. Liu, et al. 2024. "*Valsa mali* Effector Vm_04797 Interacts With Adaptor Protein MdAP-2β to Manipulate Host Autophagy." *Plant Physiology* 195: 502–517.

Sundstrom, J. F., A. Vaculova, A. P. Smertenko, et al. 2009. "Tudor Staphylococcal Nuclease Is an Evolutionarily Conserved Component of the Programmed Cell Death Degradome." *Nature Cell Biology* 11: 1347–1354.

Vargason, J. M., G. Szittya, J. Burgyan, and T. M. Hall. 2003. "Size Selective Recognition of siRNA by an RNA Silencing Suppressor." *Cell* 115: 799–811.

Wang, N., C. Tang, X. Fan, et al. 2022. "Inactivation of a Wheat Protein Kinase Gene Confers Broad-Spectrum Resistance to Rust Fungi." *Cell* 185: 2961–2974.e2919.

Wang, W., J. Nie, L. Lv, et al. 2021. "A *Valsa mali* Effector Protein 1 Targets Apple (*Malus domestica*) Pathogenesis-Related 10 Protein to Promote Virulence." *Frontiers in Plant Science* 12: 741342.

Wang, W., S. Wang, W. Gong, et al. 2022. "*Valsa mali* Secretes an Effector Protein VmEP1 to Target a K Homology Domain-Containing Protein for Virulence in Apple." *Molecular Plant Pathology* 23: 1577–1591.

Xu, M., Y. Guo, R. Z. Tian, et al. 2020. "Adaptive Regulation of Virulence Genes by microRNA-Like RNAs in *Valsa mali*." *New Phytologist* 227: 899–913.

Yang, C., Y. Yu, J. Huang, et al. 2019. "Binding of the *Magnaporthe oryzae* Chitinase MoChia1 by a Rice Tetratricopeptide Repeat Protein Allows Free Chitin to Trigger Immune Responses." *Plant Cell* 31: 172–188.

Yang, W., T. P. Chendrimada, Q. Wang, et al. 2006. "Modulation of microRNA Processing and Expression Through RNA Editing by ADAR Deaminases." *Nature Structural & Molecular Biology* 13: 13–21.

Yin, C., S. R. Ramachandran, Y. Zhai, C. Bu, H. R. Pappu, and S. H. Hulbert. 2019. "A Novel Fungal Effector From *Puccinia graminis* Suppressing RNA Silencing and Plant Defense Responses." *New Phytologist* 222: 1561–1572.

Yin, Z., H. Liu, Z. Li, et al. 2015. "Genome Sequence of Valsa Canker Pathogens Uncovers a Potential Adaptation of Colonization of Woody Bark." *New Phytologist* 208: 1202–1216.

Zhang, H., M. Gao, W. Zhao, and L. Yu. 2023. "The Chromatin Architectural Regulator SND1 Mediates Metastasis in Triple-Negative Breast Cancer by Promoting *CDH1* Gene Methylation." *Breast Cancer Research* 25: 129.

Zhang, P., Y. Jia, J. Shi, et al. 2019. "The WY Domain in the *Phytophthora* Effector PSR1 Is Required for Infection and RNA Silencing Suppression Activity." *New Phytologist* 223: 839–852.

Zhang, T., Y. L. Zhao, J. H. Zhao, et al. 2016. "Cotton Plants Export microRNAs to Inhibit Virulence Gene Expression in a Fungal Pathogen." *Nature Plants* 2: 16153.

Zhang, X., Y. R. Yuan, Y. Pei, et al. 2006. "Cucumber Mosaic Virus-Encoded 2b Suppressor Inhibits *Arabidopsis* Argonaute1 Cleavage Activity to Counter Plant Defense." *Genes & Development* 20: 3255–3268.

Zhao, J. H., and H. S. Guo. 2022. "RNA Silencing: From Discovery and Elucidation to Application and Perspectives." *Journal of Integrative Plant Biology* 64: 476–498.

Zhu, C., J. H. Liu, J. H. Zhao, et al. 2022. "A Fungal Effector Suppresses the Nuclear Export of AGO1-miRNA Complex to Promote Infection in Plants." *Proceedings of the National Academy of Sciences of the United States of America* 119: e2114583119.

Supporting Information

Additional supporting information can be found online in the Supporting Information section.